We are IntechOpen,
the world's leading publisher of
Open Access books
Built by scientists, for scientists

6,900
Open access books available

186,000
International authors and editors

200M
Downloads

154
Countries delivered to

Our authors are among the

TOP 1%
most cited scientists

12.2%
Contributors from top 500 universities

CLARIVATE ANALYTICS
BOOK CITATION INDEX
INDEXED

WEB OF SCIENCE™

Selection of our books indexed in the Book Citation Index
in Web of Science™ Core Collection (BKCI)

Interested in publishing with us?
Contact book.department@intechopen.com

Estimation of Excess Pore Pressure Generation and Nonlinear Site Response of Liquefied Areas

Kamil Bekir Afacan

Abstract

Recent studies about liquefaction initiation are widely encountered in the literature in terms of utilizing the dynamic triaxial tests under harmonic loading and site response of liquefied zones. Sandy-like or clayey-like behavior is important for estimating the liquefaction susceptibility but there are other factors related to cyclic loading characteristics such as frequency content and stress level. Besides, 1-D ground response analyses are employed to understand the behavioral transmission through the soil column in liquefiable areas. The study here focuses on two main aspects of the liquefaction. The first part consists of the estimating of the pore pressure generation under irregular excitations, whereas the second part aims to assess the efficiency of the building codes predicting the nonlinear site response in liquefied prone areas. The laboratory results show that the frequency content has big influence on the liquefaction at varying stress levels. Moreover, literature models have discrepancies to estimate the pore pressure generation under different types of loading. Regarding the site response, it was indicated that equivalent linear approach is incapable of predicting the seismic behavior of soil column; therefore, nonlinear ground response must be run instead, and the IBC is the most effective one to match the nonlinear analysis results.

Keywords: liquefaction, pore pressure generation, nonlinear site response, dynamic soil behavior, building codes

1. Introduction

Liquefaction is one of the most important and complex topics that geotechnical engineers deal with in today's practice. The Good Friday (Alaska) and Niigata (Japan) earthquakes in 1964 are the very first earthquakes that the destructive effect of the liquefaction was observed as the slope failures, bearing failures of foundations and abutments, etc. It has been studied widely since, and so many researchers have helped liquefaction to be understood better although the topic is still complicated in many sense. The initiation of the studies starts in the 1960s by Seed and his colleagues. Seed and Ldriss in 1967 [1], Seed in 1968 [2], and Seed and Peacock in 1971 [3] set the base of the liquefaction concept by studying the clean sand samples to evaluate the cyclic resistance of the soils, and Finn et al. [4, 5], Castro [6, 7], and Youd [8, 9] are other examples that focused on the liquefaction around that time.

Cyclic loading of the saturated coarse soils causes excessive pore pressure buildup under undrained conditions. This excessive pore pressure can converge up to the total stress; meaning zero effective stress is described as liquefaction [10]. It means that the soil is no longer capable of carrying any load resulting in soil failures and/or excessive deformations of structure foundations. Therefore, this phenomenon is very crucial to take into consideration in designing a structure in liquefaction susceptible areas.

The process of the pore pressure buildup mainly depends on the wave propagation throughout the soil column that is excited by an earthquake. Loose soils tend to densify when they are loaded under drained conditions, whereas if the condition happens to be undrained, the compression of the soil during cyclic loading is almost impossible. In this case, there is not enough time for water to escape from the voids; therefore it takes the seismic load reflecting as increase in the pore pressure. This pore pressure starts building up until the loading is finished. If the energy created by the excitation is big enough, the amount of the pressure will finally reach to the total stress. Since there is no effective stress anymore, the soil grains will escalate in the water and lose its strength therefore stability. Thus, the liquefaction susceptibility should be questioned in seismic areas with some basics: Is the soil coarse and loose enough for being susceptible to liquefy? Is the region active enough to produce sufficient energy to liquefy the soil? If so, does the liquefaction happen in shallow depths that will greatly affect the superstructure on it, or does it happen very deep that nothing will be felt on the ground? These are the questions that should be answered in seismically active regions to take initial precautions for possible hazards.

Although the liquefaction susceptibility is correlated with the in situ test results (SPT, CPT, Vs) or soil index parameters (relative density, fine content, Atterberg limits, etc.) in practice, today's technology gives engineers big confidence to run laboratory cyclic tests in order to understand the behavior of the soil under seismic loads. It is understandable to use empirical models to evaluate the liquefaction; because of its easiness, they are not as accurate as the real scale pore pressure models observed by the dynamic triaxial tests conducted in the laboratory. The complexity of the excess pore pressure generation models is still there, but it is the most appropriate way to estimate the dynamic behavior of coarse soils. Since the correlations do not give any information about the pore pressure generation, the possible deformations on the ground due to liquefaction is not more than an approach for them; however, the level of deformation levels can be observed in the laboratory rigorously [11]. It should also be noted that the tests can be run in varied strain amplitudes (10^{-6}–10^{0}).

The cyclic behavior of soils is commonly determined by the dynamic triaxial test equipment in the laboratory. Pore pressure generations models are mainly studied into three different approaches: (i) stress-based models, (ii) strain-based models, and (iii) energy-based models. The purpose of stress-based models is to relate the excess pore pressure ratio (r_u) which is the normalization of the excess pore pressure by the effective stress with the number of cycles to liquefy the soil. Lee and Albaisa [12] and Seed et al. [13] studied the relation between the r_u with (N/N_{liq}) where N is the number of loading cycle and N_{liq} is the number of cycle to initiate liquefaction. Later, Booker et al. [14] worked in the same model but offered different constants, and Polito et al. [15] in 2008 came up with a model consisting of fine content, relative density, and cyclic stress ratio. Finally, Baziar et al. [16] updated the formulation with some new parameters. Regarding the strain-based models, the change in volumetric strain is estimated with the cyclic shear strain along with some constants for the clean sand samples [4, 5, 16, 17]. More complex models were introduced by Dobry et al. [18–20], Vucetic and Dobry [21], and Carlton [22] with

new parameters such as threshold cyclic shear strain, the dimension of the loading and other fitting parameters in relation to fine content, shear wave velocity, etc. Energy-based models focus on the stress-strain loops to calculate the enough energy to estimate the liquefaction susceptibility, and Green et al. [23] is one the most widely used models in this concept. In this study, the laboratory tests were conducted at different cyclic stress ratios (CSR), and the results were compared with the stress-based models. The details of these models and their formulation will be discussed later.

As mentioned before, loss of stiffness of soil is a big problem for civil engineers. Kramer et al. [24] states that estimation of the soils behavior under dynamic loading is crucial to construct any kind of structures reliable and economical. Other than laboratory studies, building codes regulate the design for a structure to be built in a specific region to estimate the dynamic loads that will be transmitted throughout the soil layers to the structure for some seismic scenarios. Ground response varies a lot with the dynamic behavior of soils and local site conditions under seismic activity. The building codes generally construct the response spectrum differently with regard to the soil class which is determined by the shear wave velocity of upper 30 m. The classification of this kind misses the local site effects on the ground response that the structure will be exposed to. Therefore, the site-specific response plays an important role to estimate the dynamic loads propagated to the soil surface. Building codes generally set some rules to necessitate the site response (i.e., ZF soil class); however, the prediction of the dynamic loads that structure would feel will change drastically by the nonlinearity of soil behavior.

Dynamic behavior of soils is obtained in the laboratory conducting dynamic triaxial tests for medium to high and resonant columns test for low to medium shear strain levels. The behavior is modeled with the modulus reduction and damping properties of soil at varying shear strains. These values are evaluated from the stress-strain loops for every cycle to build two important curves presenting the soil nonlinearity.

This chapter will outline the liquefaction studies into two groups which will be (i) experimental and (ii) analytical approaches. Initiation of the excess pore pressure buildup resulting r_u = 1 ends up as liquefaction of soil, and it can mainly be assessed in the laboratory by the dynamic triaxial test systems. Eighteen different dynamic tests were conducted at different CSRs and loading types in order to obtain the pore pressure generation and validate the models in the literature with the recorded data. The second part of the study will focus on the nonlinear site response of the liquefied areas with the available in situ data. Five different boring logs were used in the analyses, and the nonlinear behavior of the soil layers was determined for each. It should be noted that all the soil columns were liquefied at different depths for different earthquake scenarios. The ground responses were calculated, and finally the performance of the building codes to estimate the spectral response of the soil columns was assessed.

2. Estimation of the excess pore pressure generation

In this part, clean sand samples were loaded under varying cyclic stresses with different loading patterns using the dynamic triaxial test system equipped at the Eskisehir Osmangazi University Soil Dynamics Laboratory, and it is presented in **Figure 1**.

The system is a fully automated pneumatic system that is capable of conducting axial strains up to 10%, and the tests can be handled as stress controlled or strain controlled. A total of 18 tests was completed to justify the performance of the excess pore pressure generation models suggested in the literature.
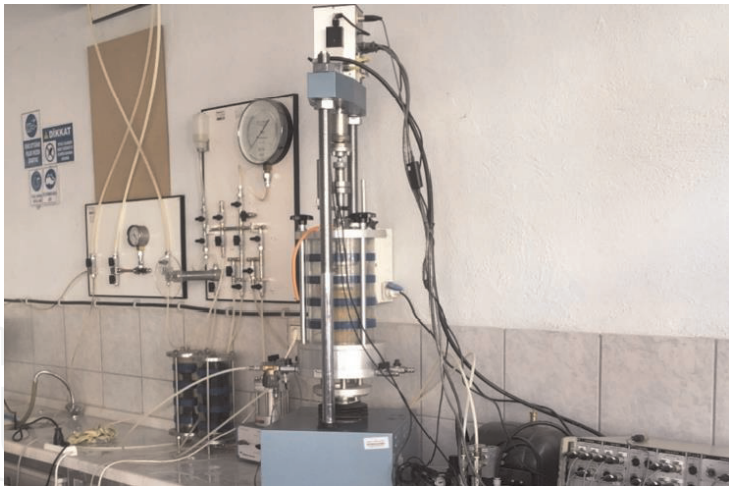
Figure 1.
Dynamic triaxial test system at the Eskisehir Osmangazi University.

2.1 Material and method

In order to study liquefaction in the laboratory, standard sand samples are generally chosen for the tests since the cost of the undisturbed sand samples that is only possible by the freezing technique are really high. Therefore, clean Podima sand samples were used in this study. The type of sand is classified as poorly graded sand (SP) according to the unified soil classification system (USCS), and the grain size distribution is shown in **Figure 2**. The minimum and maximum unit weights of the sand were determined as 15.30 and 17.66 kN/m^3 as the standards suggest, respectively. The specific gravity was determined as 2.63.

The soil samples had a diameter of 7 cm and a height of 14 cm, and the desired relative density was decided to be as 40%. Dried sand was dropped into a two parted mold, which has a membrane placed in, by a funnel with some little shaking and compacting of the sample accordingly. Later, the top header was set on the sample, and some vacuum was applied to the sample in order to hold itself, and the mold was taken apart. Following external cell placement, the cell was
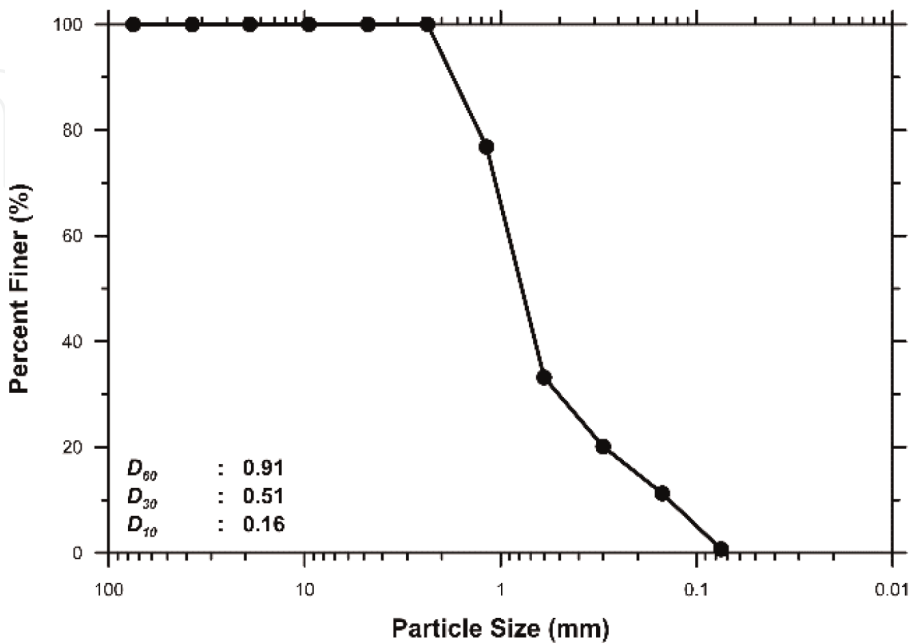

Figure 2.
Grain size distribution of the sand used in the study.

filled with water, and some cell and back pressures were applied in such a way that there was a difference of 5 kPa at increasing level. The saturation was controlled with the B constant to reach a value of 0.96. After saturation was accomplished, the sample was consolidated under isotropic condition approximately an hour with a confining pressure of 65 kPa. Finally, soil samples were axially loaded at different amplitude of stresses with changing loading shapes until all the samples were liquefied.

2.2 Test program and loading patterns

In order to understand the excess pore pressure generation at different cyclic stresses, three different stress levels were considered. Cyclic stress ratio is defined as the cyclic stress applied to the sample (either compression or extension) normalized by the confining pressure, and they were assigned as 0.15, 0.20, and 0.30 for the test program. All the samples were confined by the cell pressure of 65 kPa. The text program is shown in **Table 1**.

As seen in the table, a total of 18 tests was programmed to see the effect of the stress level and loading characteristics. It is customary to use harmonic loading in the liquefaction studies; however, irregular loading shapes were used in this study to investigate the differences. Six different patterns were used to axially load the samples, and the double amplitude of axial stresses was kept constant at each CSRs. The loading shapes at CSR = 0.20 level are presented in **Figure 3**.

2.3 Excess pore pressure generation models

Since the tests were assessed as stress controlled, the stress-based models were chosen to measure their performance with the laboratory results. Four different equations suggested by the models are presented in **Table 2**.

In the table, N is the specific cycle that the excess pore pressure ratio to be calculated and N_L is the number of cycles that liquefies the soil. α is a fitting constant, and although Seed and Booker propose as it is taken to be 0.7, Polito et al. advanced this constant with other parameters such as fine content (FC), relative density (D_r), and CSR. More complex model was offered by Baziar in 2011 with two different constants θ and β. These constants differ with the content of the silt in the sandy soil. Since clean sand samples were tested in this study, only related constants are shown in the table. The model Booker proposed gives almost identical results as Seed et al.'s model does; therefore it is not presented in the following part.

2.4 Observations

A total of 18 cyclic triaxial tests was planned to gather excess pore pressure generation at different stresses with changing excitation patterns. Using the necessary information from the test data, the excess pore pressure ratios (r_u) which were the ratio of the excess pore pressure recorded during cyclic loading over the

CSR	Double amp. axial str. (kPa)	Type 1	Type 2	Type 3	Type 4	Type 5	Type 6
0.15	20	X	X	X	X	X	X
0.20	26	X	X	X	X	X	X
0.30	39	X	X	X	X	X	X

Table 1.
Test program in terms of stress levels and loading types.
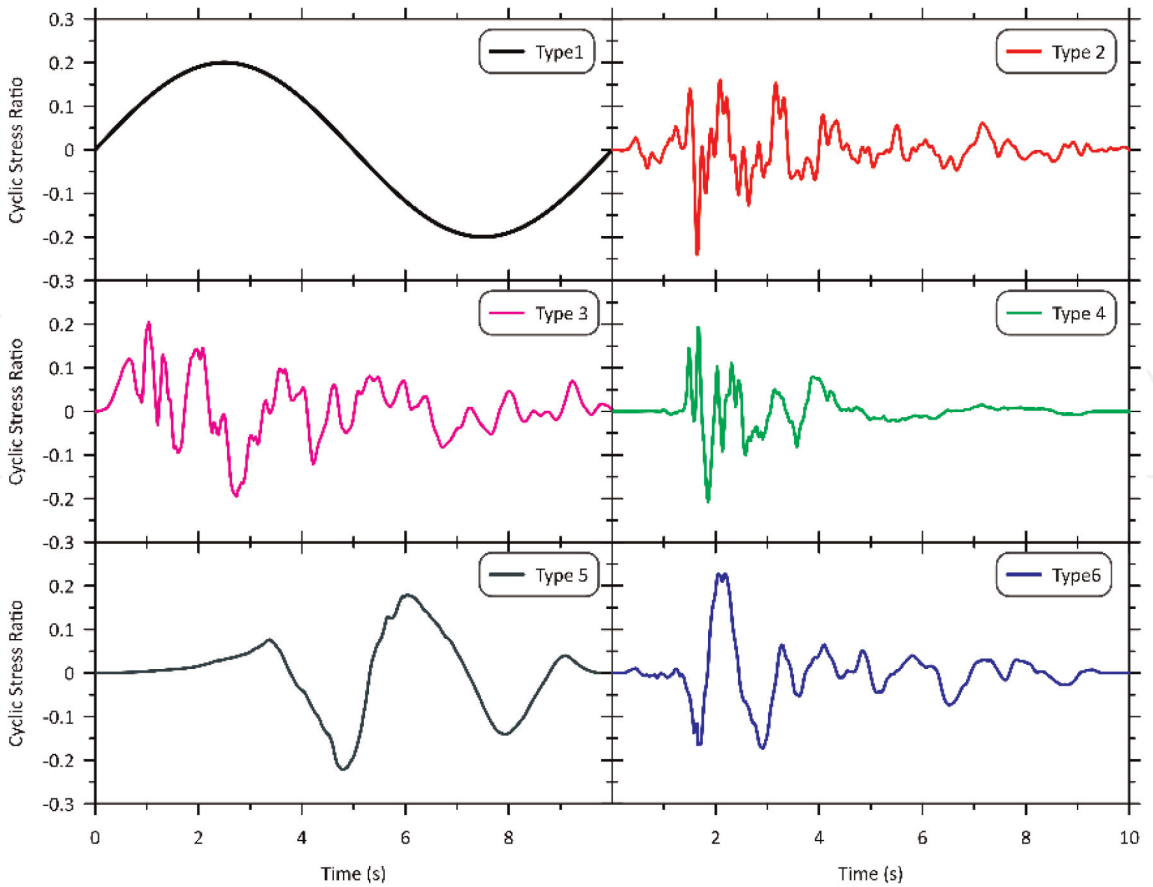
Figure 3.
Example loading shapes at the level of CSR = 0.20.

Models	Equation	Notes
Seed et al. [13]	$r_u = \frac{1}{2} + \frac{1}{\pi} \sin^{-1}\left[2\left(\frac{N}{N_L}\right)^{1/a} - 1\right]$	$\alpha = 0.7$
Booker [14]	$r_u = \frac{2}{\pi} \sin^{-1}\left[\left(\frac{N}{N_L}\right)^{1/a}\right]$	$\alpha = 0.7$
Polito et al. [15]	$r_u = \frac{2}{\pi} \sin^{-1}\left[\left(\frac{N}{N_L}\right)^{1/a}\right]$	$\alpha = 0.01166 \cdot FC + 0.007397 \cdot D_r$ $+ 0.01034 \cdot CSR + 0.5058$
Baziar [16]	$r_u = \frac{2}{\pi} \sin^{-1}\left[\left(\frac{N}{N_L}\right)^{1/2\theta}\right] + \beta\sqrt{1 - \left\{\frac{2N}{N_L} - 1\right\}^2}$	$0.6 \leq \theta \leq 0.8$ $0.0 \leq \beta \leq 0.25$

Table 2.
Models and associated equations used to compare the test results.

confining pressure of 65 kPa were calculated for the models mentioned in the previous section. The test data and corresponding models proposed by Seed et al. [13], Polito et al. [15], and Baziar [16] at CSR = 0.15 are presented in **Figure 4**.

The first thing to point out in the figure is that the liquefaction happens in various times for different types of loading, although the double amplitude axial stresses are the same for all the six tests. The longest time to liquefy the clean sand sample happened to be almost 18,500 seconds for the sinusoidal type of loading, whereas this duration came out to be in an interval of 3500–8600 seconds for irregular type of loading. As seen in the upper left side of the figure, the recorded pore pressure buildup differs a lot with regard to other types. An initial increase was recorded in a short time, and it fluctuated for almost 10,000 seconds, and then the
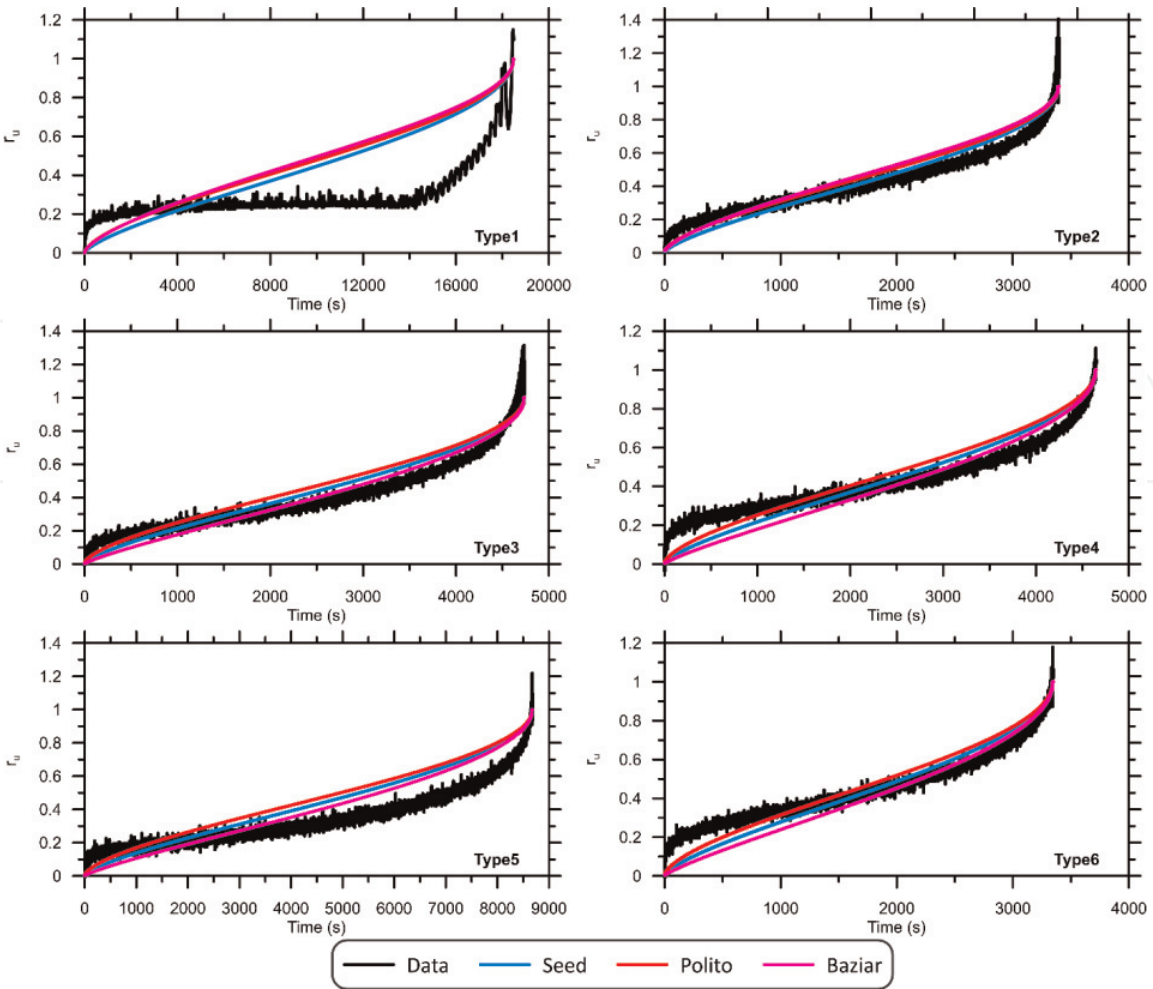
Figure 4.
Excess pore pressure ratios for the test data and models at CSR = 0.15.

accumulation of the excess pressure started to increase again, and then liquefaction finally occurred after 5000 seconds for Type 1. Similar trends were observed for the rest of the tests for shorter periods.

Regarding the models suggested in the literature, they do not behave much different at this stress level. Although they did not do a good estimation to represent the data gathered from the sinusoidal loading, other pore pressure ratios along time were predicted alright by the models, being slightly on the conservative side. It should be noted that all three models missed the initial increases in pore pressure regardless of type of loading. Lastly, the pore pressure observed from the type five loading acts more like a harmonic loading than irregular type of loading, and models overestimated the pore pressure generation after 2000 seconds until the liquefaction developed. Overall, some model has better presentation of the observed data at certain type of loading, and some does at others. Therefore, no model perfectly matches with the test data.

Moving on to the higher stress level, **Figure 5** shows the recorded excess pore pressure ratios at CSR = 0.20 for six different tests and corresponding estimations by the literature models. Compared to the lower stress level, the liquefaction initiation did not take that long under cyclic stress ratio of 0.20. It occurred around 130–420 seconds for soil to lose its stability for irregular types of loading, whereas it took almost 2.5–8 times longer for soil to liquefy under harmonic loading. The literature models ideally followed the pore pressure record gathered from the three tests under loading of Type 3, Type 5, and Type 6; Baziar, being the best, did acceptable predictions for other two tests (Type 2 and Type 4 loadings).
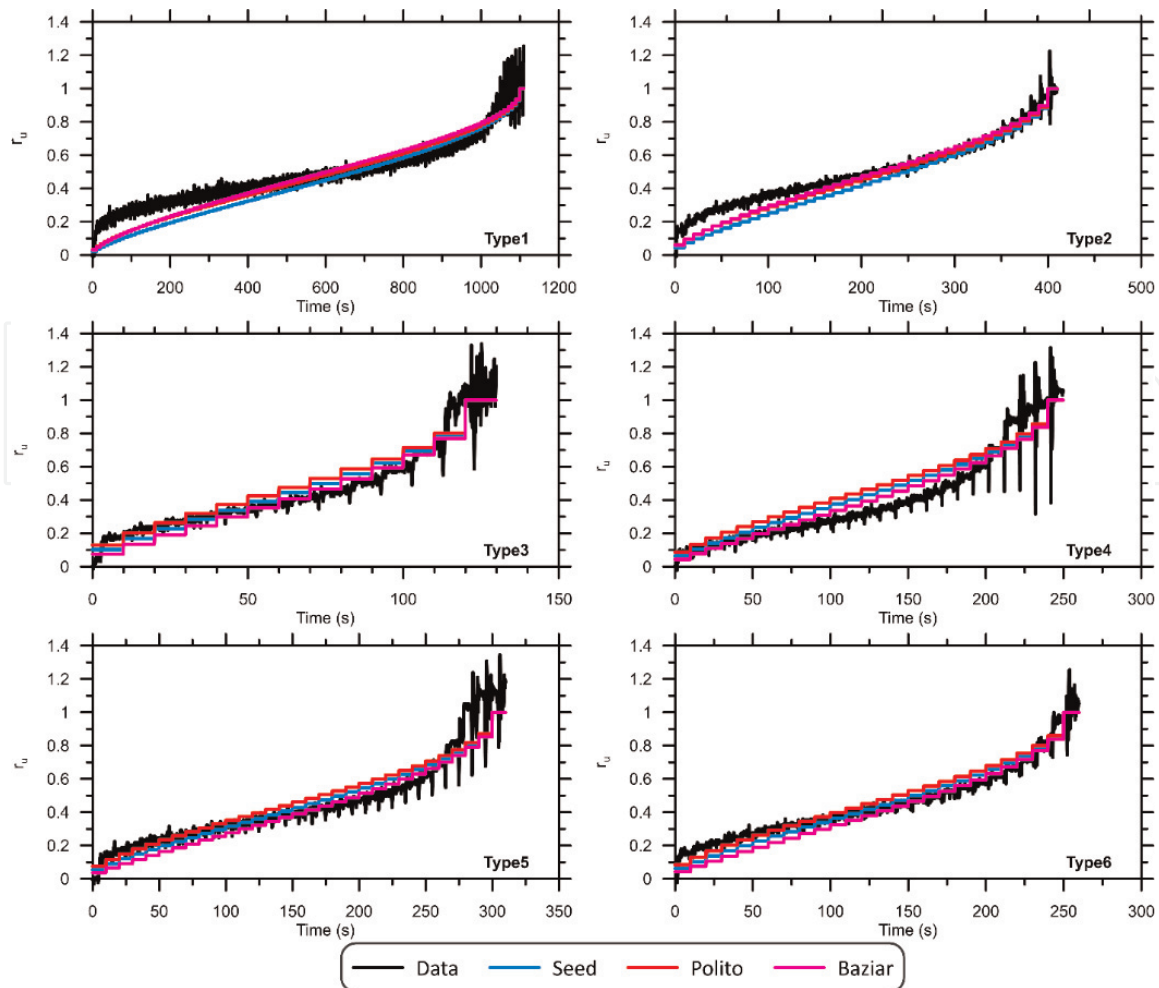
Figure 5.
Excess pore pressure ratios for the test data and models at CSR = 0.20.

As the axial stress increases, the pore pressure buildup behavior under sinusoidal loading converges to the one loaded by the irregular type. There is still a mismatch at the initial, but after 400 seconds, all three models presented the data alright for the Type 1 loading. It is obvious that most of the time the model proposed by Baziar [16] is the closest to the recorded data, and Polito's model [15] gives the upper limit out of the three models, whereas the other model stayed in between two.

Final set of tests were carried out at a high stress (CSR = 0.30) and recorded excess pore pressure ratios over time, and corresponding literature predictions are presented in **Figure 6**. It is obvious that the increasing stress level causes soil to liquefy at low number of cycles. For all the types of loading, it did take only 1–10 cycles for soil to lose its rigidity meaning not more than 100 seconds. As seen in the figure, all of the literature models predicted the pore pressure generation almost perfectly for the test done using Type 2 loading. Regarding the others, the data are underestimated by all the models especially the test data observed from the harmonic loading. It is hard to estimate the performance of the models to represent the data under Type 5 loading since it took only 1 cycle (10 seconds) to liquefy the soil.

There is one question that can arise to understand the behavior of the liquefaction occurred when harmonic loading was applied: Did the soil liquefy at 100 seconds or earlier like 30 seconds where the first time r_u value reached 1.0? During the specific test, the deformation of the soil was carefully observed with the naked eye along with the computer screen. Although r_u came to 1.0 around 30 seconds, the soil was not totally unstable and still was able to resist more loads. Therefore, the total stability lost was waited to terminate the test, and it lasted almost 100 seconds.
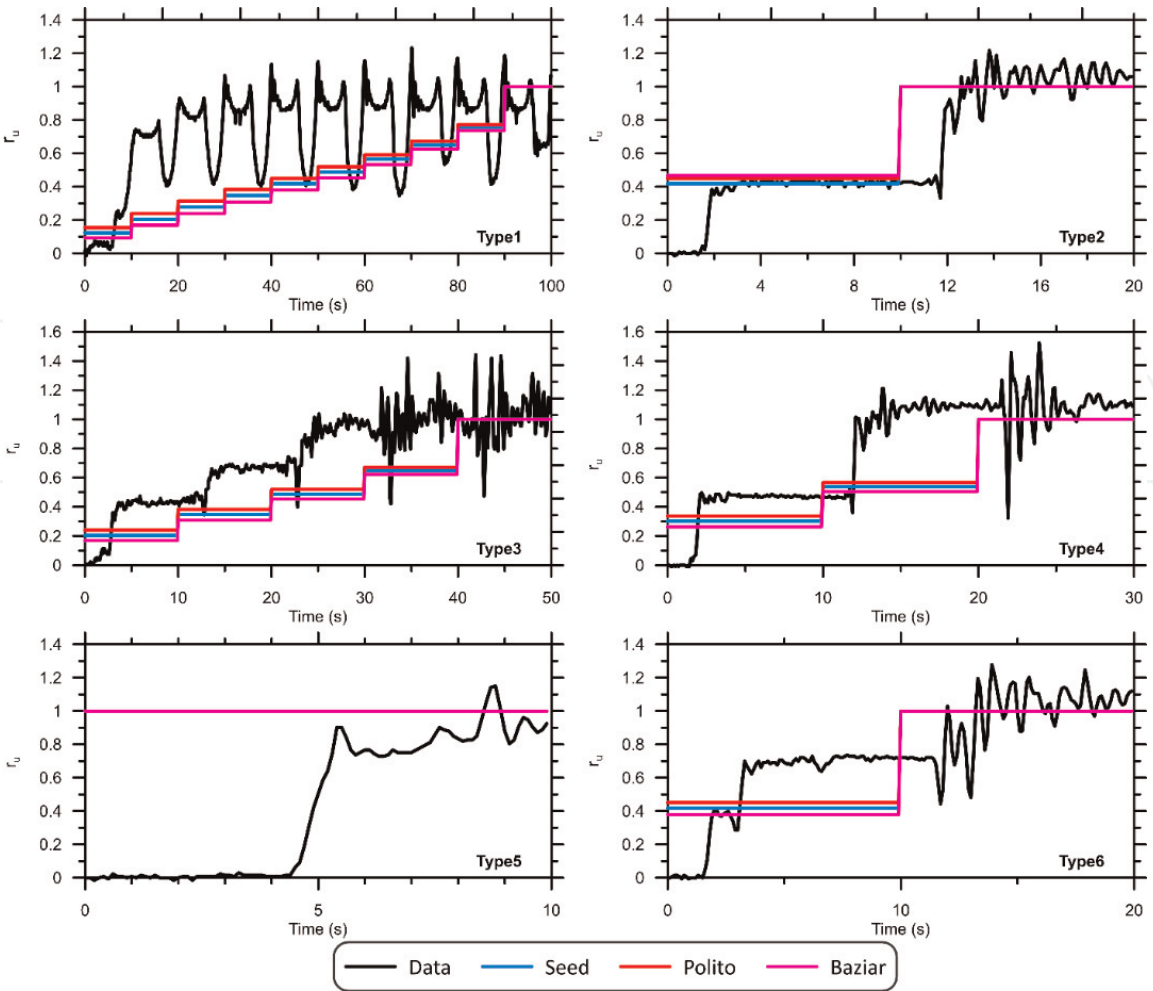
Figure 6.
Excess pore pressure ratios for the test data and models at CSR = 0.30.

2.5 Discussion

Out of 18 cyclic triaxial tests to understand the soil liquefaction susceptibility, it is observed that the shape of the loading or in other words frequency content of the excitation plays an important role to cause instability. Earthquakes are never harmonic types of excitations, and using sinusoidal loading in order to understand the soils dynamic behavior may mislead the interpretation. **Figure 7** explains how many
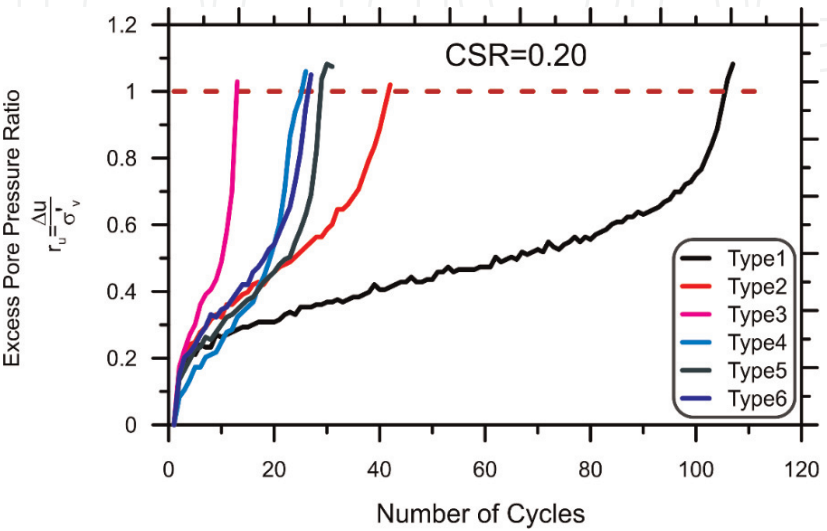
Figure 7.
The effect of loading on the change of number of cycles to liquefy soil.

cycles are needed to liquefy soil sample for different types of loading at a double amplitude of 26 kPa stress, just to give an example.

One clear point can be made from the figure that the variety of loading and its dominant frequency are effective on the number of cycles that would initiate the liquefaction. Although the excess pore pressure buildups are similar for the first 5 cycles, Type 1 with the harmonic shape diverges from the rest of the group, and the number of cycles needed for liquefaction occurs to be at least 2.5 times later than the others. With regard to the irregular type of loadings, they even act differently, and the number of cycles to liquefy the soil varies between 10 and 40 which can be considered a wide interval. Thus, the potential of liquefaction triggering should be studied with different types of loading when needed.

The essence of the results in terms of number of cycles to liquefy soil samples is shown in **Tables 3** and **4**.

It should be noted that the variation is a lot for different cyclic stress ratios. For example, Type 3 and Type 4 loading patters need similar number of cycles to liquefy the soil at CSR = 0.15, whereas it changes for increasing CSRs. Harmonic loading always takes more time/cycle to generate pore pressure than others, and every irregular loading type has its varying frequency-dependent characteristics at increasing stresses. Therefore, the excess pore pressure generation is not only affected by the frequency content of the loading alone, but also the stress levels along with it play important role in estimating liquefaction triggering.

As a summary, three different stress levels at varying loading shapes were used to run dynamic triaxial tests in order to determine the generation of excess pore pressures under cyclic excitations. The desired relative density and confining pressure for all 18 tests were constant as 40% and 65 kPa, respectively. There are a few clear points that are worth to emphasize:

i. The pattern of the loading (harmonic vs. inharmonic) is an effective parameter that influences the duration and the number of cycles to liquefy same soil samples.

ii. As the stress level increases, the number of cycles for soil to lose its stability decreases. For example, the needed time to liquefy soil at CSR = 0.15 changes

CSR	Type 1	Type 2	Type 3	Type 4	Type 5	Type 6
0.15	1848	340	474	466	867	335
0.20	111	41	13	25	31	26
0.30	10	2	5	3	1	2

Table 3.
Number of cycles to initiate liquefaction for different types of loading.

Boring	Depth (m)	V_s (m/s)	$V_{s,30}$ (m/s)	FC (%)
B1	20	150–280	220	10–85
B2	20	180–190	185	5–42
B3	20	165–290	230	27–35
B4	20	145–195	175	8–32
B5	20	165–175	170	18–38

Table 4.
Soil profiles.

to between 3500 and 18,500 seconds, and these values drop to 130–1100 seconds at CSR of 0.20. Even a small difference in the applied stress amplitude may cause a drastic drop in the number of cycles.

iii. There are many stress-based models to estimate the pore pressure buildup in the literature, and three of them were used here to see their performance to estimate the laboratory data. Models have better representation of the pore pressure generation at the low to medium stress levels for irregular loading patterns, and at high stress levels the capability to estimate the data is not that well. Among the models, the model Baziar et al. [16] suggests relatively does better jobs, and Polito et al.'s [15] model is being on the safer side all the time. However, the performance of all three to predict the recorded data does not differ that much.

iv. The dynamic triaxial tests take some time to set the sand sample appropriately and evaluate the data to understand the behavior, but other levels of relative densities and confining pressures should be tested to have better understanding of the pore pressure generation concept.

v. The latest point is that the effect of fine content should also be investigated, and if the opportunities (budget, facility, etc.) are possible, undisturbed samples should directly be taken out of the site to see if the real in situ samples are represented well by the laboratory approaches in order to evaluate the response of the pore pressure buildup.

3. Nonlinear site response of liquefied areas

3.1 Introduction and studied area

Japan, Chile, the USA, Italy, Iran, and Turkey are some of the most important earthquake-prone countries, and they have been exposed to devastating activities over the last decades causing damaged buildings and many fatalities. One of the most essential regions for liquefaction studies in the literature is the Duzce/Sakarya Region in Turkey which was immensely affected by Kocaeli and Adapazari (Duzce) earthquakes in 1999. Liquefaction susceptibility in structural design should be considered in zones consisting of loose sand soils because it may cause significant damages as excessive settlement and sinking of the structures. This can only be possible by the nonlinear site-specific analysis.

In this section, the nonlinear site response of liquefied areas will be investigated using the well-documented in situ data taken from the city of Sakarya which is surrounded by Istanbul, Yalova, Duzce, and Bilecik. The region lays on the extension of the North Anatolian Fault Zone [25], and it is neighboring two local faults (Sapanca and Duzce), and the map is presented in **Figure 8**. The area suffered a lot, and many liquefied zone were inspected during Duzce Earthquake in 1999.

Five different boring log data were used in the analyses to evaluate the ground response in a liquefied prone zone. The soil profiles consist of almost 90% of silty sands (SM), and some low-plasticity clays, gravelly sands, and clayey sands can be found in very shallow depths. A summary table showing the information about the logs is presented below.

All the borings are 20 m long having shear wave velocity (V_s) values changing from 145 to 290 m/s. The average V_s of upper 30 m for each profile was also determined to be able to use it in the estimation of the surface response spectra
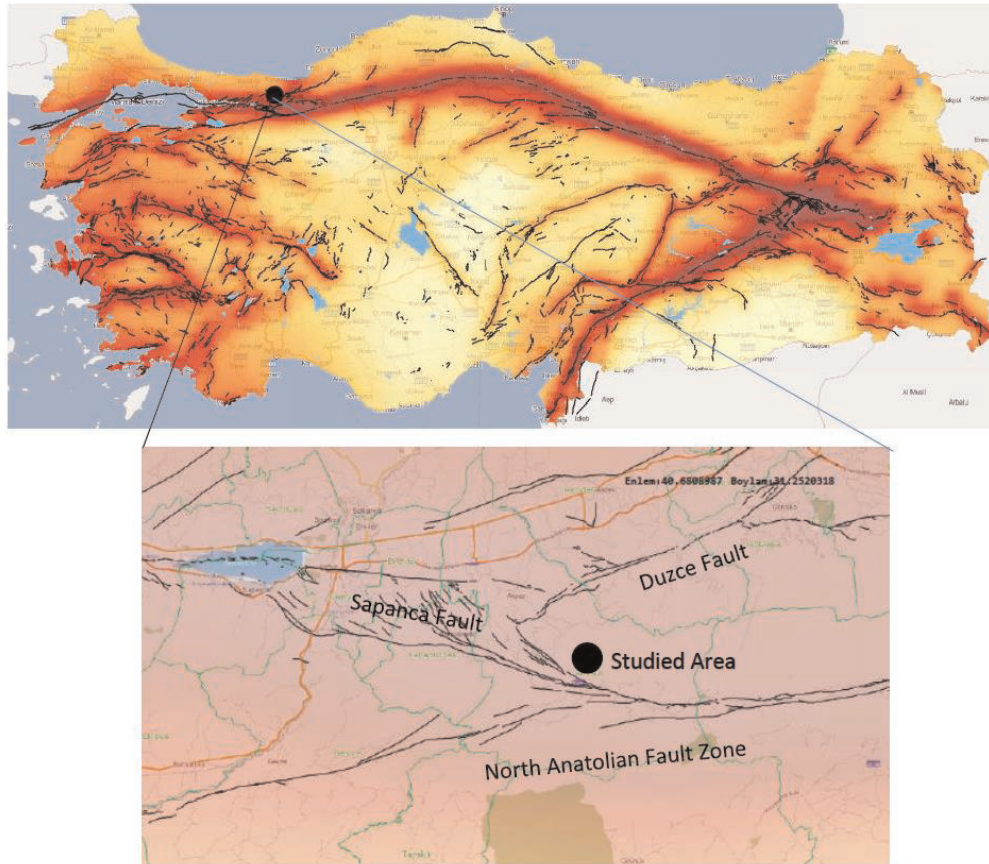
Figure 8.
Studied area and the active fault lines [29].

offered by the building codes, and the soil type of two borings is classified as ZE, and three of them are ZD. The fine content for the layers were obtained as well, and the variation is listed in the table. Layers have water content of 11–25%, and the unit weight of the soils samples laid in a range of 17.6–18.9 kN/m^3 throughout the profiles. Some triaxial tests were run in the laboratory to evaluate the strength of the sandy soils, and 33–38 degrees of friction angle along with 0–5 kPa cohesion were detected.

The dynamic properties (modulus reduction and damping behavior of soils at varying strains) of clays and sands were calculated adopting proposed models by Darendeli [26]. During the analyses, pore pressure generation was let to build up during cyclic loading in nonlinear analyses; however it was not possible by the frequency-dependent equivalent linear simulations. With the available information of the soil index properties, the required parameters were derived to model the pore pressure generation behavior suggested by Matasovic and Vucetic [27].

3.2 Motions used in the analyses

Building codes generally split possibility of earthquake levels into some groups, and the two of them have extensive use in geotechnical and earthquake engineering which are: (1) 2% chance of being exceeded in 50 years and (2) 10% chance of being exceeded in 50 years. They offer different response spectrum envelopes for each with the help of regional earthquake maps for the seismic design. To be used in the analysis, the possible local peak ground acceleration (PGA) was determined as 0.720 g for the studied area from the seismic maps which was just published in March 2018 by the Disaster and Emergency Management Authority (AFAD) under the Ministry of Interior in Turkey. Three different earthquakes happened in last

20 years (Duzce, Kocaeli, and Van earthquakes) were chosen to produce possible regional earthquake scenarios. The details of the earthquakes used in the process are shown in **Table 5**.

All of the earthquakes can be considered as the big magnitude earthquakes as seen in the table. Two of the events were taken from the Pacific Earthquake Engineering Research Center (PEER) [28] and one from the Strong Motion Data Base of Turkey (SMDB-TR) [29], and all of them were scaled to the local PGA accordingly. **Figure 9** shows the scaled versions of the earthquakes, in other words possible earthquake schemes for the studied area for the probability of 10% chance of being exceeded in 50 years.

The duration of the earthquakes differs from 25 to 85 seconds, and PGAs were set to be 0.72 g for all of them. More high-frequency content is seen from top to

Earthquake	Year	Source	Station	Magnitude	R_{jb} (km)
Duzce	1999	PEER	Duzce	7.1	0
Kocaeli	1999	PEER	Izmit	7.5	1.38
Van	2011	SMDB-TR	Van	6.7	19.2

Table 5.
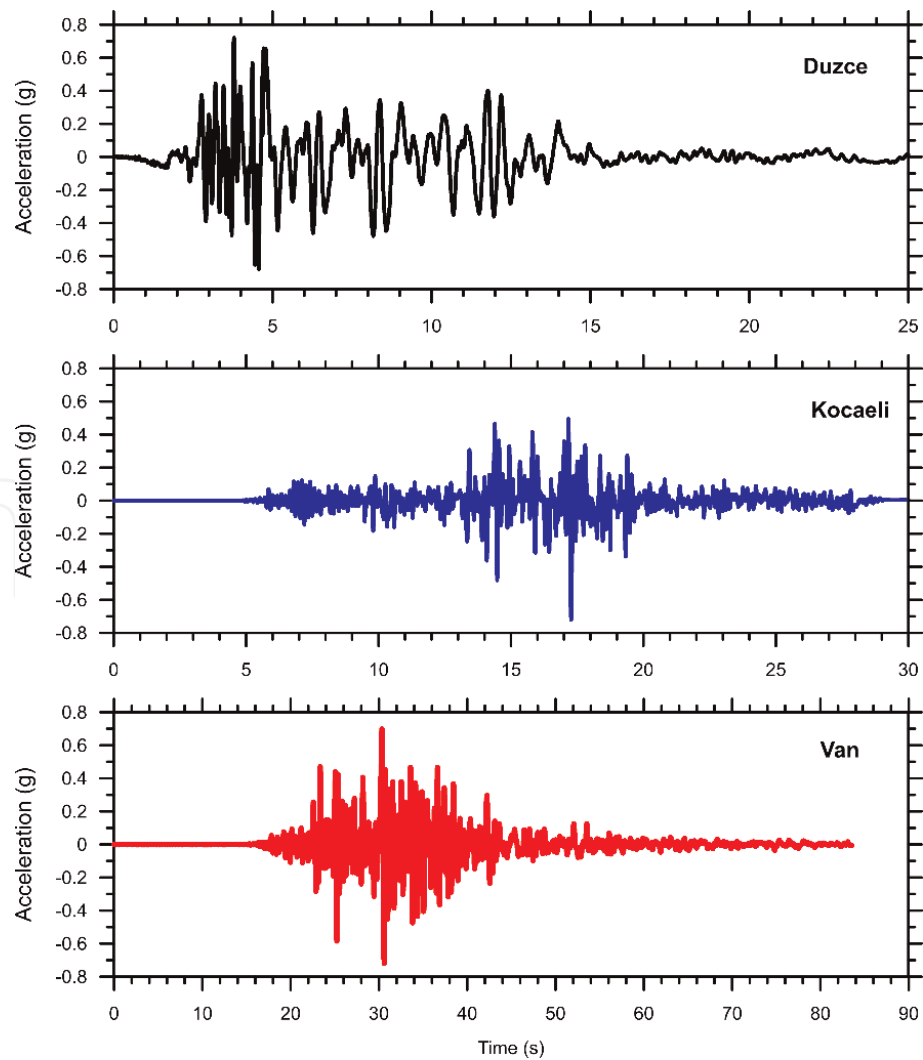*Reference earthquakes used in the analysis.*

Figure 9.
Scaled versions of the earthquake data.

bottom of the figure, and these records were used as the base motions in the analyses.

3.3 Results of a specific soil profile

Site response analyses were conducted using DEEPSOIL [30] program version 6.1, and to be able to compare different approaches, five borings were excited at their base with three shakings with nonlinear and equivalent linear models for a total of 30 analyses. The results for the boring B1 shook by Duzce record, an example set, were presented in **Figures 10–12** showing the NL and EL model estimations for the surface acceleration, their corresponding spectral behavior on
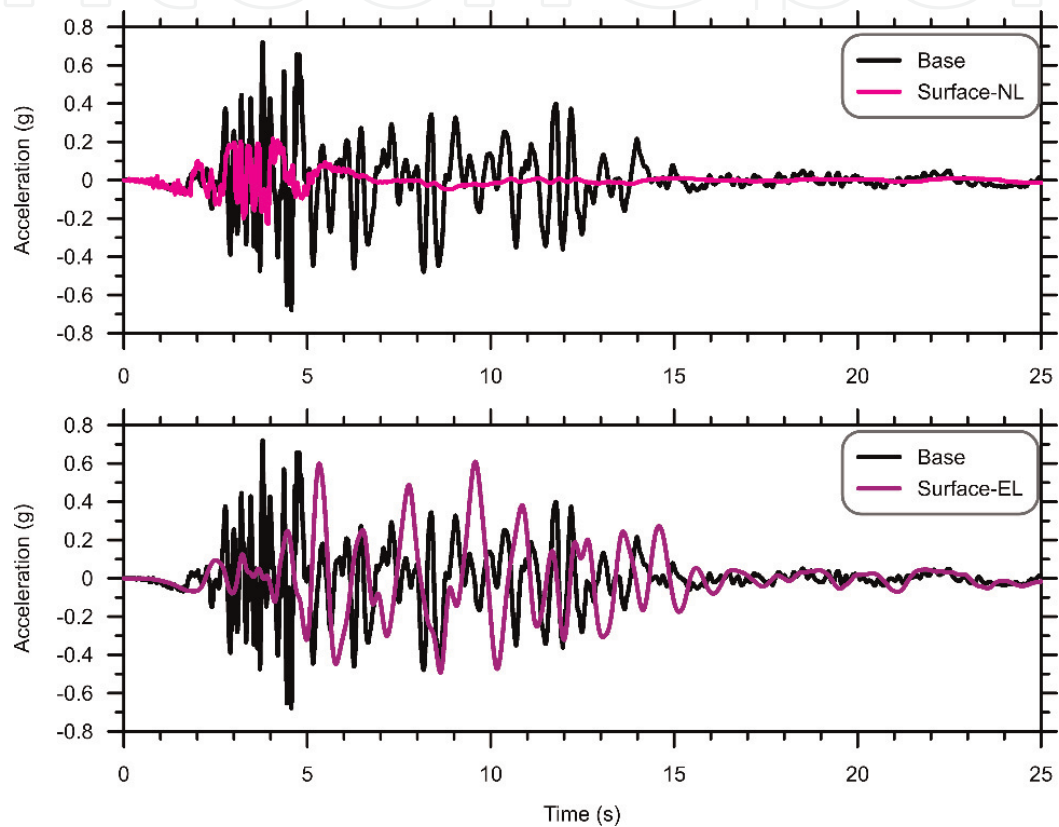
Figure 10.
Base and surface acceleration observed from the nonlinear (NL) and equivalent (EL) linear models.
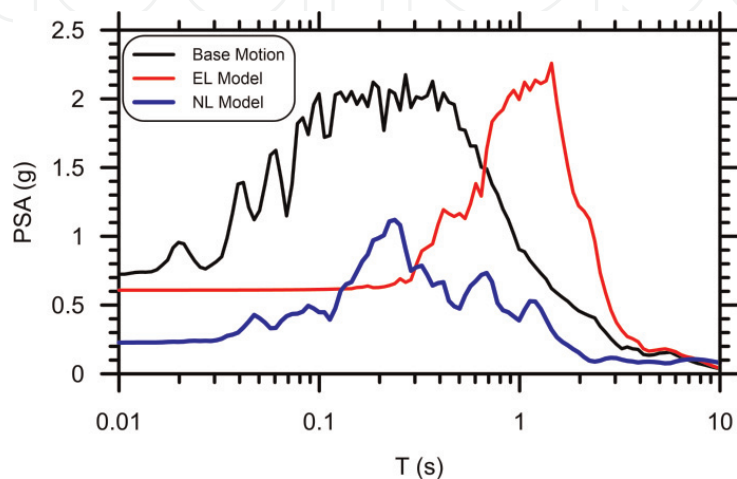
Figure 11.
Spectral acceleration of the base and the surface calculated from the NL and EL models.

the ground and the peak spectral accelerations, and maximum shear strains throughout the soil profile, respectively.

Regarding the surface acceleration predicted by two different approaches, there is a big deviation in the peaks and the time they occur. NL model shows that soil totally de-amplified the energy exerted by the motion, and the peak ground acceleration was noted around 0.25 g, whereas the peak-based acceleration was 0.72 g, and the main peaks happened around the similar time interval (3–5 seconds). However, an entirely different case was observed for the EL model. The prediction of the peak surface acceleration happened to be around 10 seconds extending the peak-based motion to 5–6 seconds, and not much de-amplification was noticed. In order to evaluate this behavioral diversity, the spectral acceleration at the surface was presented below.

The peak-based spectral acceleration (around 2 g) stays in a wide range of period between 0.1 and 0.8 seconds as seen in the figure. The NL model has compressed the behavior in terms of the size of peak ground and peak spectral accelerations. The model lessens the spectral acceleration 2–2.5 times at any period, whereas the EL model lengthened the peak spectral range to 0.9–1.8 seconds with almost no change in the amplitude. Another point about the EL model is that the initial flat part lasts longer than the base and NL model prediction. The last figure of the example set is the variation of the peak spectral acceleration and maximum shear strains through the soil column, and it is presented in **Figure 12**.

The difference between the models to estimate two parameters is concrete as observed from the figure. The peak-based acceleration was amplified a bit between 10 and 20 m and then de-amplified some for the rest of the profile by the EL model, whereas it was weakened all over the soil profile by the NL model. The soil profile was separated into three divisions, and it is supported by the related maximum shear strains at the same depths. It is obvious that two definite soil failures happened at the 8 m and 14 m according to the NL model, whereas the soil failures
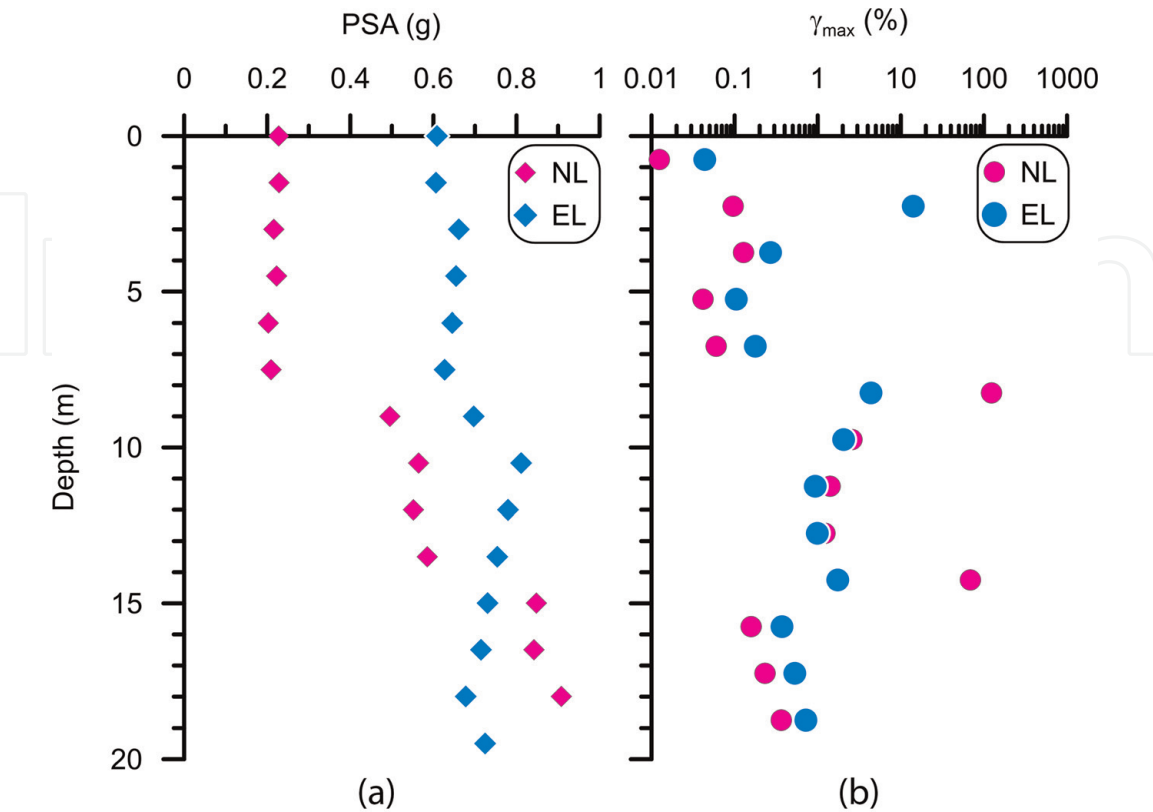

Figure 12.
Peak spectral accelerations and maximum shear strains throughout the soil columns for the NL and EL models.

seem to be predicted at the depth of 2 m and 8 m by the EL model. There are still other local failures between 9 and 13 m, but the deformation level is limited compared to the ones mentioned above. It can be concluded that not only the ground response predicted by two models is quite distinct, but also the seismic actions alter the seismic behavior extremely along the soil column.

3.4 Interpretation of the analyses

The loss of soil stiffness can be caused by either insufficient bearing capacity or liquefaction triggered by the excess pore pressure generated under cyclic loading. Thus, it is beneficial to see the pore pressure generation if it was the origin of excessive deformations during seismic excitations that only NL models are capable to investigate. Excess pore pressure ratio which is a value between 0 and 1 is one vital criterion in evaluation of the liquefaction. r_u of 1 means that the soil layer is under risk to liquefy for such type of loading. **Figure 13** shows the excess pore pressure ratios projected by the NL models for all the logs.

One clear remark can be pointed out here that the liquefaction occurring at various depths in different logs considering all three base motions sets out the possible explanation of the unreasonable deformation indicated in the previous figure. The NL model did not anticipate liquefaction triggering for the shallow depths which include some fine content, whereas there are at least nine points that soil layers mainly composed by silty sands are expected to lose their strength due to liquefaction for such sequence of events. The r_u value is greater than 0.8 for approximately 45 points meaning that even if there is no liquefaction initiated yet, soil would possibly lose its strength at these depths. Therefore, soil mitigation would be needed for possible construction in the area.

After liquefaction assessment of the soil profiles, the next step is to evaluate the site response in terms of nonlinear and equivalent linear approaches. Fifteen different analyses were conducted for each, and the peak spectral accelerations on the surface are presented in **Figures 14** and **15**. As mentioned before, building codes
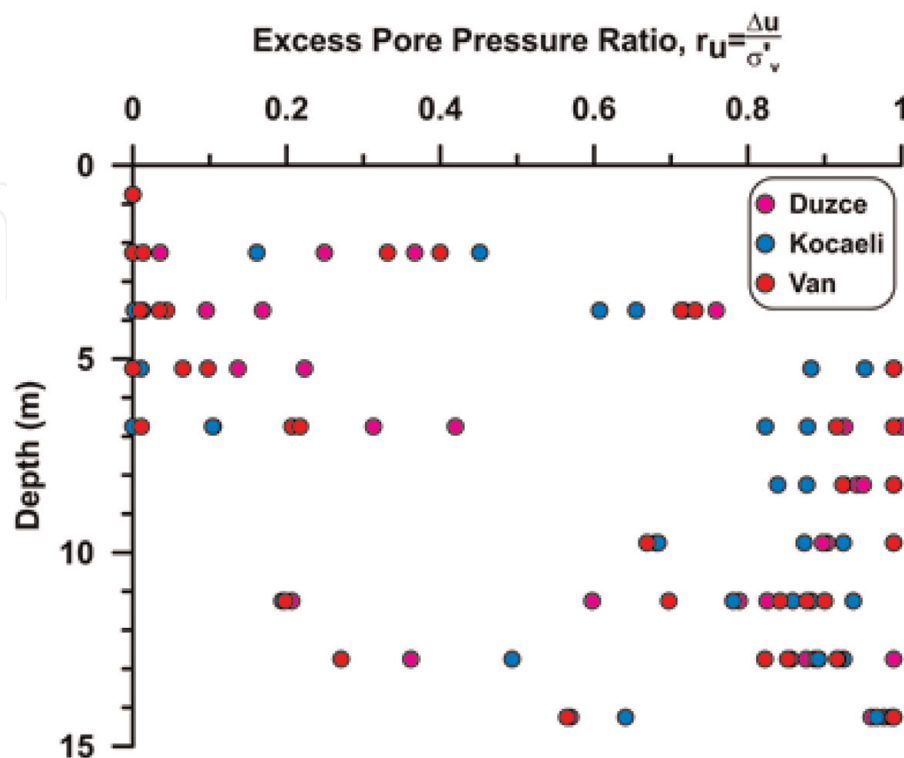

Figure 13.
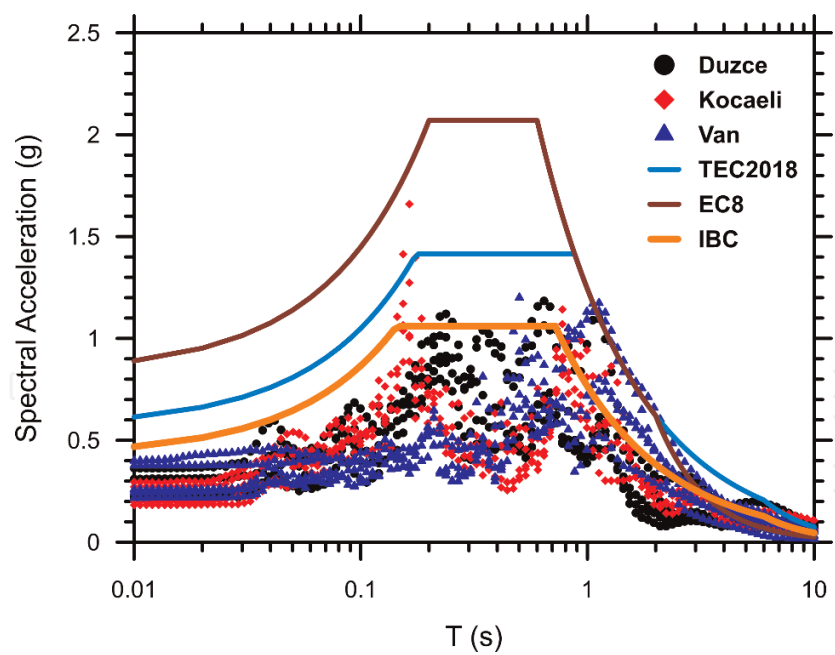*Excess pore pressure ratios estimated from 15 NL analysis.*

Figure 14.
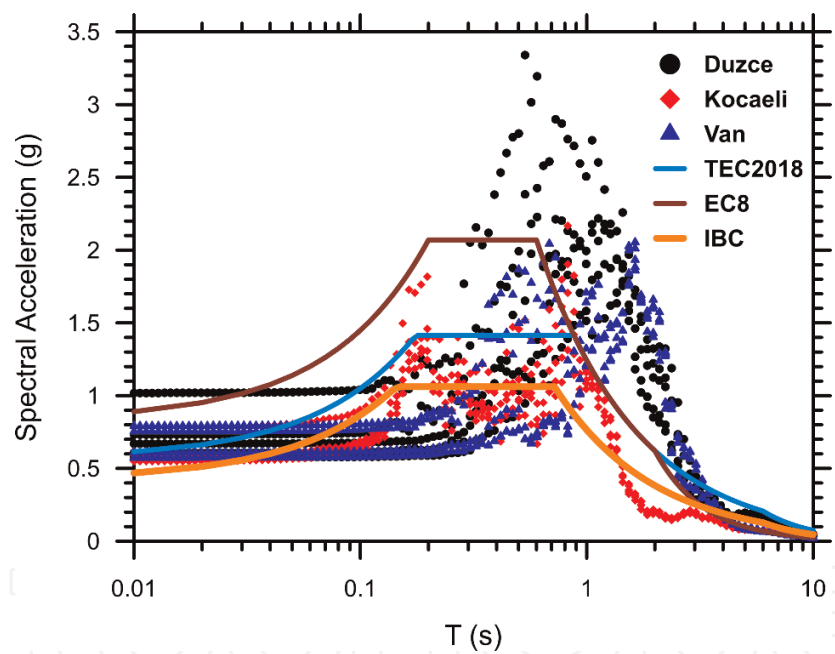*Ground responses evaluated from the NL analysis and building codes' design spectra.*

Figure 15.
Ground responses evaluated from the EL analysis and building codes' design spectra.

rule out the possible designs with seismic maps and some regulations. In order to see if they are good representatives of the site, corresponding response spectrum envelopes were evaluated using the new Turkish Building Code (TBC2018), Eurocode8 (EC8), and International Building Code-ASCE 7.05 (IBC), and they are shown in figures along with the ground response spectra gathered from the analyses.

Considering the PGAs, the variation is almost 100% from one log to another (0.20–0.40 g) in such a small area. The trend of the spectral accelerations is similar for increasing period; however the amplitudes differ a lot especially the change in peak spectral accelerations between 0.1 and 1 seconds. The lowest is reported as 0.3 g, whereas the highest is around 1.2 g with one outlier with the red dots. It is a bit off compared to the rest of the data; therefore it can be excluded to represent the general picture of the area.

In terms of the performance of the building codes with regard to expressing the site specifics, all of them are on the safer side (EC8 is the most conservative one and the IBC is the least) following the similar flow of spectral acceleration of the observed data from the nonlinear analyses. IBC's spectra would be considered as the most economical one compared to the others with missing some longer period content, and it would possibly be a better representation if the flat part of the spectra shifted on the right (by using larger corner periods). About the TEC2018, the spectra at higher period were estimated better, but the content from small to medium periods would not be cost-effective in the seismic design. As seen in the figure, EC8 envelope is not practical at all, and such design would be the most expensive one among three building codes.

Equivalent linear analyses are easy to perform with less parameter needed to constitute a site and widely used in the practice and literature. However, one should be cautious to use this approach in such cases. Since this frequency-based analytical approach is not suited for liquefaction analyses, the results may canalize the engineer to an inappropriate design. Although the details of the results obtained from the equivalent linear analyses will not be covered here, it is important to call attention to the differences. The spectral acceleration of 15 analyses is presented in **Figure 15** with their corresponding envelopes suggested by building codes.

As seen in the figure, the soil amplified the base motion and lengthened it to the higher periods for these earthquake scenarios. None of the building codes were capable of expressing the data very well, neither the peak spectral acceleration nor the corner frequencies. However, it should be underlined here that it is not the performance of the building codes, but instead it is the analytical approach of the equivalent linear analysis lacking to model the excess pore pressure generation and the damping behavior of the soil. Thus, nonlinear site-specific response in liquefied areas is crucial in the design, and the concept of liquefaction susceptibility should be explained more clearly in the building codes.

4. Conclusions

Pore pressure generation under cyclic loading is an important phenomenon for liquefaction triggering, and the number of cycles and/or duration to liquefy soil is affected a lot by the frequency content of the loading. Three different stress levels were tested at varying loading patterns, and it can be concluded that harmonic loading to estimate the liquefaction initiation is not that reliable in order to evaluate the dynamic behavior of sands. Regarding the number of cycles, it took almost 1848 cycles to liquefy the sand samples which is at least two times later than Type 5 loading, and this value goes up to 5.5 times at most for Type 6 at CSR = 0.15. The same comparison at CSR level of 0.20 shows that the shortest time to trigger liquefaction is 130 seconds, whereas it lasted 1110 seconds for harmonic loading being almost nine times later. Even among the irregular loading types, the difference was calculated as 2.5–3 times in terms of the number of cycles for soil to lose its stability at different stress levels. Therefore, frequency content and its link with the CSR level are of great importance on excess pore pressure buildup. With reference to the stress-based models in the literature to estimate the recorded data in the laboratory, the mentioned models were not that distinct to predict the data, and it was noted that the best prediction was noticed at the medium stress level (CSR = 0.2). Moreover, the model proposed by Baziar [16] had a better job presenting the test data than the other two.

Though nonlinear site response is a bit complicated to gather enough information to simulate the ground response, it is the most appropriate way to model the

seismic behavior in liquefied zones. The in situ data was taken from Duzce area which was liquefied in 1999 in Adapazari earthquake, and the nonlinear analyses helped reproduce the liquefaction triggering at 45 points in different depths for varying earthquake scenarios. Since the equivalent linear approach cannot perform the liquefaction triggering, it alters the transmission of the shear waves affecting the spectral accelerations and the maximum shear strains throughout the soil layers. It was noted that the PSA was estimated as three times larger at shallow depths with corresponding shear strains as an example. Consequently, it should not be used for ground response in liquefaction-prone areas not to misinterpret the dynamic behavior of soils. Compared to three building codes to project the site response, the International Building Code is the most effective one to match the nonlinear analysis results.

Finally, it can be summarized that frequency content is highly effective on excess pore pressure buildup; the variation of its impact at different stress levels should not be disregarded in dynamic triaxial testing; and granting all this complexity of the nonlinear site-specific analyses, designers must be encouraged to run nonlinear analyses to model soil behavior better for safer superstructures, and the building regulations should be improved in terms of liquefaction susceptibility.

Author details

Kamil Bekir Afacan
Eskisehir Osmangazi University, Eskisehir, Turkey

*Address all correspondence to: kafacan@ogu.edu.tr

IntechOpen

References

[1] Seed HB, Idriss IM. Analysis of soil liquefaction: Niigata earthquake. Journal of the Soil Mechanics and Foundations Division. 1967;**94**(SM3):83-108

[2] Seed HB. Landslides during earthquakes due to soil liquefaction. Journal of the Soil Mechanics and Foundations Division. 1968;**93**(SM5): 1053-1122

[3] Seed HB, Peacock WH. Test procedures for measuring soil liquefaction characteristics. Journal of the Soil Mechanics and Foundations Division. **97**:1099-1119

[4] Finn WDL, Lee KW, Martin GR. An effective stress model for liquefaction. Journal of the Geotechnical Engineering Division. 1977;**103**(GT6):517-533

[5] Finn WDL, Ledbetter RH, Wu G. Liquefaction in Silty Soils: Design and Analysis, Ground Failures under Seismic Conditions, Geotechnical Special Publication 44. New York: ASCE; 1994. pp. 51-76

[6] Castro G, Poulos SJ. Factors affecting liquefaction and cyclic mobility. Journal of the Geotechnical Engineering Division. 1977;**106**(GT6):501-506

[7] Castro G. On the behavior of soils during earthquakes—Liquefaction. In: Proceedings, NSF/EPRI Workshop on Dynamic Soil Properties and Site Characterization; EPRI NP-7337; Vol. 2; Palo Alto, California: Electric Power Research Institute; 1991. pp. 1-36

[8] Youd TL, Hoose SN. Liquefaction susceptibility and geologic setting. In: Proceedings, 6th World Conference on Earthquake Engineering; New Delhi; Vol. 3, 1977. pp. 2189-2194

[9] Youd TL. Geologic effects-liquefaction and associated ground failure. In: Proceedings, Geologic and Hydrologic Hazards Training Program. Open File Report 84-760, U.S. Geological Survey; Menlo Park, California; 1984. pp. 210-232

[10] Seed HB, Tokimatsu K, Harder LF, Chung RM. Influence of SPT procedures in soil liquefaction resistance evaluations. Journal of Geotechnical Engineering. 1985;**Ill**(12):1425-1445

[11] Kwan WS, Sideras S, El Mohtar CS, Kramer S. Pore pressure generation under different transient loading histories. In: Tenth U.S. National Conference on Earthquake Engineering Frontiers of Earthquake Engineering Anchorage; Alaska; 2014

[12] Lee KL, Albaisa A. Earthquake induced settlements in saturated sands. Journal of the Soil Mechanics and Foundations Division. 1974;**100**(GT4)

[13] Seed HB, Idriss IM, Makdisi F, Banerjee N. Representation of Irregular Stress Time Histories by Equivalent Uniform Stress Series in Liquefaction Analyses, EERC 75-29. Earthquake Engineering Research Center, University of California: Berkeley; 1975

[14] Booker JR, Rahman MS, Seed HB. A computer program for the analysis of pore pressure generation and dissipation during cyclic or earthquake loading. Berkeley: Earthquake Engineering Center, University of California; 1976

[15] Polito CP, Green RA, Lee J. Pore pressure generation models for sands and silty soils subjected to cyclic loading. Journal of Geotechnical and Geoenviromental Engineering. 2008; **134**(10):1490-1500

[16] Baziar MH, Shahnazari H, Sharafi H. A laboratory study on the pore pressure generation model for Firouzkooh silty sands using hollow

torsional test. International Journal of Civil Engineering. 2011;**9**(2):126-134

[17] Byrne PM. A model for predicting liquefaction induced displacement. In: Proceedings, 2nd International Conference on Recent Advances in Geotechnical Earthquake Engineering and Soil Dynamics; St. Louis, Missouri; Vol. 2. 1991. pp. 1027-1035

[18] Dobry R, Ladd RS. Discussion to soil liquefaction and cyclic mobility evaluation for level ground during earthquakes, by H.B. Seed and Liquefaction potential: Science versus practice, by R.B. Peck. Journal of the Geotechnical Engineering Division. 1980;**106**(GT6):720-724

[19] Dobry R, Ladd RS, Yokel FY, Chung RM, Powell D. Prediction of Pore Water Pressure Buildup and Liquefaction of Sands during Earthquakes by the Cyclic Strain Method, NBS Building Science Series 138. Gaithersburg, Maryland: National Bureau of Standards; 1982. 150 p

[20] Dobry R. Mohamad R. Dakoulas P. Gazetas G. Liquefaction evaluation of earth dams—A new approach. In: Proceedings, 8th World Conference on Earthquake Engineering; Vol. 3; 1984. pp. 333-340

[21] Vucetic M, Dobry R. Effect of soil plasticity on cyclic response. Journal of Geotechnical Engineering. 1991;**117**(1): 87-107

[22] Carlton B. An improved description of the seismic response of sites with high plasticity soils, organic clays, and deep soft soil deposits [thesis]. Berkeley: University of California; 2014

[23] Green RA, Mitchell JK, Polito CP. An energy-based pore pressure generation model for cohesionless soils. In: Proceedings: John Booker Memorial Symposium; 16–17 November 2000; Melbourne, Australia; 2000

[24] Kramer S, Hartvigsen AJ, Sideras SS, Ozener PT. Site response modeling in liquefiable soil deposit. In: 4th IASPEI/IAEE International Symposium. Effect of Surface Geology on Seismic Motion; 2011

[25] Komazawa M, Morikawa H, Nakamura K, Akamatsu J, Nishimura K, Sawada S, et al. Bedrock structure in Adapazari, Turkey—A possible cause of severe damage by the 1999 Kocaeli earthquake. Soil Dynamic And Earthquake Engineering. 2002; **22**(9–12):829-836

[26] Darendeli MB. Development of a new family of normalized modulus reduction and material damping curves [thesis]. Austin, Texas: Department of Civil, Architectural and Environmental Engineering, The University of Texas; 2001

[27] Matasovic N, Vucetic M. Cyclic characterization of Liquefiable Sands. ASCE Journal of Geotechnical and Geoenvironmental Engineering. 1993; **119**(11):1805-1822

[28] PEER. Pacific Earthquake Engineering Research Center. Available from: https://ngawest2.berkeley.edu/

[29] AFAD. Disaster and Emergency Management Presidency Earthquake Department. Available from: http://kyhdata.deprem.gov.tr/2K/kyhdata_v4.php

[30] Hashash YMA, Musgrove MI, Harmon JA, Groholski DR, Phillips CA, Park D. DEEPSOIL 6.1, User Manual. Urbana, IL: Board of Trustees of University of Illinois at Urbana-Champaign; 2016